K-1-05

Extended Abstracts of the 2019 International Conference on Solid State Devices and Materials, Nagoya, 2019, pp449-450

High Avalanche Capability in GaN p-n Junction Diodes Realized by Shallow Beveled-Mesa Structure Combined with Lightly Mg-Doped p-Layers

*Takuya Maeda[1], Tetsuo Narita[2], Hiroyuki Ueda[2], Masakazu Kanechika[2], Tsutomu Uesugi[2], Tetsu Kachi[3], Tsunenobu Kimoto[1], Masahiro Horita[1, 3] and Jun Suda[1, 3]

[1]Kyoto University, Kyoto, 615-8246, Japan
[2]Toyota Central R&D Labs., Inc., Aichi, 480-1118, Japan
[3]Nagoya University, Aichi, 464-8603, Japan
*E-mail: maeda@semicon.kuee.kyoto-u.ac.jp

Abstract

Design and fabrication of GaN p-n junction diodes with negative beveled-mesa termination are presented. The electric field distribution in the beveled mesa edge is investigated by TCAD simulation. Based on the simulated results, the three devices with shallow-angle beveled-mesa (~10°) with various Mg acceptor concentrations in the p-layers are fabricated. All the devices showed low reverse leakage current and high avalanche capability. The increase in breakdown voltage with decreasing Mg concentrations is observed. The highest breakdown electric field of 2.86 MV/cm is achieved for the device with the breakdown voltage of 425 V.

1. Introduction

Gallium nitride (GaN) has attracted great attention as a material for the next-generation power devices owing to its high breakdown electric field (~3 MV/cm). Recently, there have been many reports on GaN vertical devices fabricated on GaN freestanding substrates [1-3].

For power devices, edge termination is key component to pull out the potential of the material. For GaN, it is challenging to form a selective p-region by Mg-ion implantation. Therefore, edge terminations without p-GaN (ex. Field plate [4, 5], Ion-implanted isolation [6], Deep trench etch termination [7]) were employed for GaN devices.

In this paper, we present design and fabrication of GaN vertical p-n junction diodes with negative beveled-mesa termination. The electric field (PNDs) distribution in the beveled-mesa edge is investigated by TCAD simulation. Based on the simulation, devices with low p-type epilayers and shallow beveled-mesa were fabricated. The fabricated GaN PNDs showed high avalanche capability. A device with lower p-type doping exhibited higher breakdown voltage, as expected from the TCAD simulation.

2. Device Design

Figure 1 shows the device structure of a GaN PND with negative beveled-mesa termination. The two-dimensional electric field distribution in the mesa edge was investigated for various epitaxial structures (doping concentrations, thicknesses) and mesa angle (θ). From the simulation, the maximum electric field (E_{max}) was obtained as an information for electric field crowding. The ratio of E_{max} to parallel-plane peak electric field (E_{pp}), which is calculated as

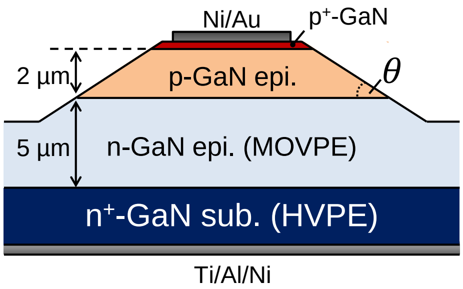

Fig. 1 Device structure of GaN-on-GaN p-n junction diode with negative beveled-mesa termination ($0 > \theta > 90°$, $N_{\mathrm{a}} > N_{\mathrm{d}}$).

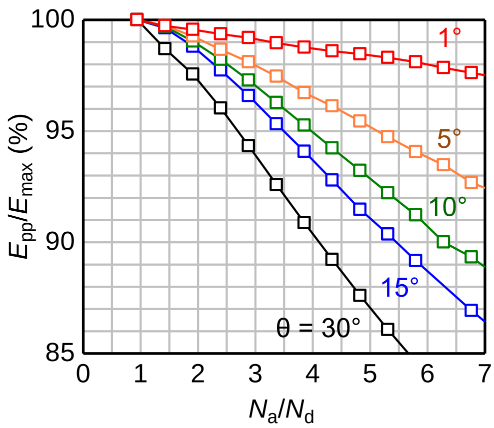

Fig. 2 The relationship between electric field crowding and the ratio of N_{a} to N_{d} for the mesa angle of 1, 5, 10, 15 and 30° for non-punch-through condition.

$E_{\mathrm{pp}} = \sqrt{2e(V_{\mathrm{d}} - V_{\mathrm{b}})/\varepsilon_{\mathrm{s}} \cdot N_{\mathrm{d}}N_{\mathrm{a}}/(N_{\mathrm{d}} + N_{\mathrm{a}})}$, is determined by $N_{\mathrm{a}}/N_{\mathrm{d}}$ and θ for non-punch-through condition.

Figure 2 shows the relationship of $E_{\mathrm{pp}}/E_{\mathrm{max}}$ vs. $N_{\mathrm{a}}/N_{\mathrm{d}}$ for mesa angle of 1, 5, 10, 15 and 30°. $E_{\mathrm{pp}}/E_{\mathrm{max}}$ comes to be close to unity with decreasing $N_{\mathrm{a}}/N_{\mathrm{d}}$ and θ. In other words, suppression of electric field crowding is obtained when N_{a} is low and θ is shallow, since low N_{a} and shallow θ extend the depletion layer at the mesa surface wider. For example, for $\theta = 10°$, $E_{\mathrm{pp}}/E_{\mathrm{max}} > 95\%$ is obtained when $N_{\mathrm{a}}/N_{\mathrm{d}} < 4$. It should be noted that the relationship does not depend on a net doping concentration $N_{\mathrm{a}}N_{\mathrm{d}}/(N_{\mathrm{a}}+N_{\mathrm{d}})$ and an applied voltage. Breakdown voltage of a device with the same θ can be increased with maintaining $N_{\mathrm{a}}/N_{\mathrm{d}}$ by changing doping concentrations, epitaxial thicknesses, and an etching depth.

Table I Doping concentration in the fabricated GaN PNDs (PN1-3) obtained from SIMS and *C-V* measurements.

	PN1	PN2	PN3
[Mg] (cm^{-3})	2.6×10^{17}	3.4×10^{17}	4.8×10^{17}
[Si] (cm^{-3})	7.0×10^{16}	6.9×10^{16}	6.9×10^{16}
[Mg][Si]/([Mg]+[Si]) (cm^{-3})	5.5×10^{16}	5.7×10^{16}	6.0×10^{16}
$N_d N_a/(N_d+N_a)$ (cm^{-3})	5.5×10^{16}	5.7×10^{16}	6.1×10^{16}

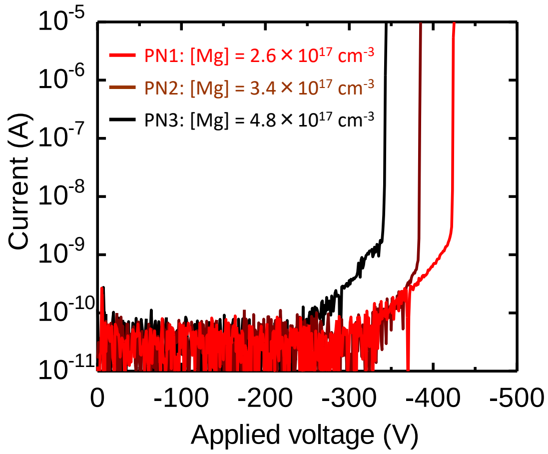

Fig. 3 Reverse current-voltage characteristics in GaN p-n junction diodes (the junction diameters are 450 μm) with Mg concentrations of 2.6×10^{17} cm^{-3}, 3.4×10^{17} cm^{-3}, and 4.8×10^{17} cm^{-3}.

3. Experimental results and Discussions

Three negative bevel GaN p-n junction diodes with shallow angle (~10°) beveled-mesa structure and various Mg concentrations were fabricated (PN1-3). The device structure is shown in Fig. 1. The 5 μm thick n-layers, 2 μm thick p-layers, and 0.2 μm thick p^+-layers were grown by metal organic vapor phase epitaxy on GaN freestanding substrates. The beveled-mesa structures were formed by Cl_2-based inductively coupled plasma-reactive ion etching (ICP-RIE) with a photoresist mask [3, 8]. The mesa height and mesa angle were 3.5 μm and 10°, respectively. The Mg concentration in p-layers, Si concentrations in n-layers obtained by secondary ion mass spectrometry (SIMS), and net doping concentrations obtained by capacitance-voltage (*C-V*) measurements are summarized in Table I.

Figure 3 shows the reverse current-voltage characteristics in PN1-PN3 with junction diameters of 450 μm. The reverse leakage current for each device was very small, indicating that the effect of the RIE-induced damage on the leakage current was small in this study. This results Breakdown voltages of 425, 385, and 345 V were obtained for PN1, PN2, and PN3 devices, respectively. Although the devices do not have any passivation structure, all the devices showed high avalanche capability; the devices does not show catastrophic breakdown and the same characteristics can be reproduced many times. These characteristics indicate that electric field crowding at the device edge and/or the mesa surface is well alleviated by the negative beveled-mesa termination.

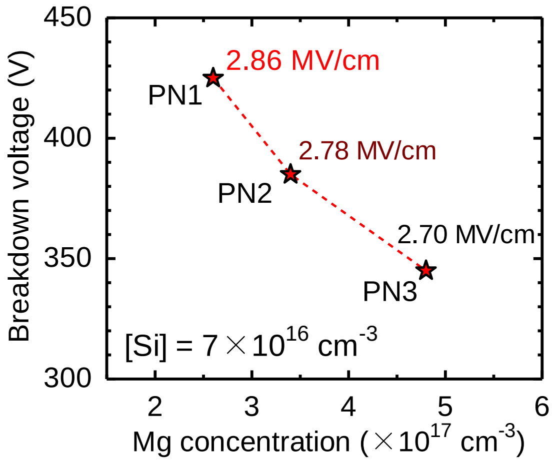

Fig. 4 Breakdown voltage vs. Mg acceptor concentration in p-layer for PN1, PN2, and PN3. The breakdown voltage increased with decreasing Mg concentration, [Mg]. The peak electric field at the breakdown for each device also increased with decreasing [Mg].

Figure 4 shows the Mg-concentration dependences of the breakdown voltage in PN1-3. The increases in the breakdown voltage and the breakdown field were observed with a decrease in Mg concentration. These results indicate that suppression of electric field crowding was obtained with decreasing Mg concentrations. This tendency shows agreement with the TCAD simulation shown in Fig.2. The highest breakdown electric field of 2.86 MV/cm was achieved for PN1 device with a breakdown voltage of 425 V. Based on the TCAD simulation, E_{pp}/E_{max} was approximately 96 %.

4. Conclusions

In this study, GaN PNDs with negative beveled-mesa termination were designed and fabricated. The breakdown voltage of the devices increased as the Mg concentration decreased. The device exhibited low reverse leakage current and high avalanche capability. For the device with the highest breakdown voltage of 425 V, a breakdown field of 2.86 MV/cm was achieved. This edge termination is useful for GaN power devices.

Acknowledgements

This work was supported by the Council for Science, Technology and Innovation (CSTI), the Cross-ministerial Strategic Innovation Promotion Program (SIP), and the Next-generation power electronics (funding agency: NEDO).

References

[1] D. Shibata *et al*., *IEDM Tech. Digest*, 2016, 10.1.1.
[2] Y. Zhang *et al*., *IEDM Tech. Digest*, 2017, 9.2.1.
[3] T. Maeda *et al*., *IEDM Tech. Digest*, 2018, 30.1.1.
[4] Y. Saitoh *et al*., *Appl. Phys. Express* **3**, 081001 (2010).
[5] K. Nomoto *et al*., *IEEE Electron Device Lett*. **37**, 2 (2016).
[6] I. C. Kizilyalli *et al*., *IEEE Electron Device Lett*. **62**, 2 (2015).
[7] H. Fukushima *et al*., *Appl. Phys. Express* **12**, 026502 (2019).
[8] F. Yan *et al*., *Mater. Sci. Forum* **389**, 1305 (2002).